ELSEVIER

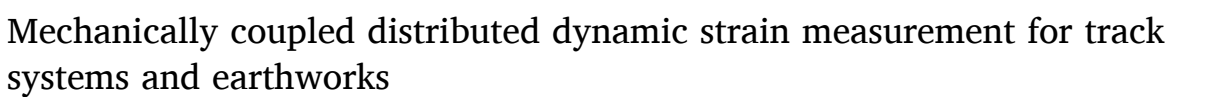
Contents lists available at ScienceDirect

Transportation Geotechnics

journal homepage: www.elsevier.com/locate/trgeo



Original Article





- ^a School of Engineering, University of Southampton, United Kingdom
- ^b Optoelectronics Research Centre, University of Southampton, United Kingdom
- ^c Network Rail, United Kingdom
- ^d Ramboll, United Kingdom

ARTICLE INFO

Keywords: Fibre Optic Sensors Railway Track Strain Measurement

ABSTRACT

Distributed optical fibre sensors are one of the few sensing technologies that could be embedded into our infrastructure to provide quantitative and mechanistic measurements of the condition of the infrastructure at network scales. This study considers the analysis of a sensing fibre deployed along 50 m of rail with a 7.5 m section buried beneath the line of the rail in the trackbed. The fibre was interrogated using a Distributed Acoustic Sensing (DAS) system based on Phase Optical Time Domain Reflectometry (\$\phi\$-OTDR). This technique offers a short gauge length and high sample rate suited for measurement of moving loads. Data were captured as the site was trafficked by passing trains. Complementary simulation and measurements (using accelerometers and pressure sensors) were used to aid and improve the interpretation of the signal from the sensing fibre. In general, the measured signal agreed with the simulation indicating that the buried fibre provides a means of measuring horizontal strain in the ground under moving loads. Results from the different measurement systems led to a consistent interpretation of site behaviour, particularly where local variation of stiffness and load distribution were detectable at the same locations along the track. These analyses support the idea that DOFS have the potential for providing quantitative and high-resolution, and hence, high-utility sensing by interrogating an optical fibre embedded in infrastructure.

Introduction

Distributed optical fibre sensors (DOFSs) have started to receive increasing attention as a technology that allows monitoring transport infrastructure by utilising optical fibres embedded into infrastructure and produce data at network scales. A single optical interrogator can monitor several tens of kilometres of sensing fibre. A variety of potential applications for DOFS systems can be realised using individual or a combination of different backscattered signals in the sensing fibre [6]. This study examines and demonstrates the application of Distributed Acoustic Sensors (DAS) mechanically coupled transport infrastructure under load, with sensing fibres installed on railway track and buried in the ground below.

Strictly, these systems are installed to measure mechanical strains but are named for their initial application, the detection of acoustic signals. The evolution of the technology has allowed strain measurement with improved linearity at low frequencies over short gauge lengths [8]. This has, in turn, made the distributed measurement of dynamic mechanical strain in a structure practicable, in a way similar to Brillouin-based DOFSs that are used for static and quasi-static strain measurement [2] or measurement based on multiple strain gauges fixed along a structure. Hence newer DAS systems can be considered as a series of overlapping strain gauges, rather than a series of microphones, used as vibration detectors. Railway-specific applications of optical fibre sensing are broad, review papers, identify applications ranging from providing operational information from train tracking to assessment of track system structural mechanical performance using sensing fibres at rail level or alongside the track [3,5,18,22].

This study is concerned with direct measurement of distributed dynamic mechanical strains due to train loading, both on the rail and in the trackbed, using a dedicated tight-buffer fibre attached to the rail and specially armoured fibre buried in the trackbed. Previous studies

E-mail address: d.milne@soton.ac.uk (D. Milne).

^{*} Corresponding author.

exploring an optical fibre mechanically coupled to a rail in the field have validate the measurement principles [23], mechanical analysis of the track system [13,15,20,24], investigating adverse performance [14] and thermal response [19]. All also these examples were limited to fibre on the rail and involved short lengths of fibre (<10 m) and very low train speeds (<5 m/s), owing to analyser and site constraints.

Here, the same system and measurement techniques described and developed in [13] are applied to a much longer stretch of railway track ~50 m, a section of which was buried in the trackbed of an operational railway. While the attachment of the fibre directly to the rail has been demonstrated and the expected signal characteristics explored, mechanical analysis for a buried fibre is a new application. The aim of this paper is to explore signal interpretation and implications for analysis of infrastructure for both fibre locations and the measurement principle for the buried fibre with reference to simulation and conventional instrumentation. The approaches demonstrated in this study are potentially applicable to measurements in other essentially elongated structures such as beams, earthworks, roads, cables and pipelines.

Background and methods

Optical measurement principle

The optical interrogator used in this study was a Distributed Acoustic Sensing (DAS) system based on Phase Optical Time Domain Reflectometry (ϕ -OTDR) developed at the University of Southampton [8,10]. For dynamic measurement optical distributed sensing, the spatial and temporal characteristics of the measurement system need to be assessed with respect to the physical characteristics of the phenomena of interest and how data is digitised for analysis. Various authors have identified up to seven system characteristics relevant for deploying a distributed optical fibre sensing system for infrastructure; these are summarised in Table 1 and illustrated in Fig. 1. Operational parameters are given in the study site section.

For distributed optical systems it is important to note that the sampling rate f_s typically refers to the rate at which the entire length of fibre can be interrogated, this influences the number of sensing channels N_{ch} along the fibre number of channels (hence their spacing) along a length L of a fibre according to the speed of the light in the fibre ν_g (the group velocity).

$$N_{ch} = \frac{L}{\frac{1}{f_s} \times \frac{V_g}{2}} \tag{1}$$

The repetition frequency, f_R determines how often each of these sensing channels are digitised and stored, akin to the convention of sample

Table 1System characteristics for mechanically coupled DOFS.

Domain	Parameter	Symbol	Description
Spatial	Sensing range	L	Length of fibre that can be mapped using a single optical interrogator
	Sampling rate	fs	The rate at which the backscattered light from entire length sensing fibre is sampled. This determines the spatial spacing between the adjacent sensing channels
	Gauge length	L_G	Length of fibre over which the net strain level is determined
	Sensing Channels	N_{ch}	Number of sensing channels along the fibre
Temporal	Repetition rate	f_R	Rate at which each sensing channel on the fibre is digitised
Measurement	Strain sensitivity Strain range		Minimum strain amplitude that can be resolved Maximum strain amplitude that can be quantified

frequency in traditional monitoring, this is usually equal to the frequency at which the optical pulses are launched into the fibre. Each optical pulse creates one OTDR trace (see the diagram at the bottom of Fig. 1). Sometimes, different names for these parameters are used in the literature [4,22]. Fig. 1 illustrates a scenario where the gauge length (which is determined by the duration of the optical pulse) is four times as long as the spatial frequency of digitizer sampling, creating an over sampling along the fibre.

Strain is measured over a length of fibre, referred to as the gauge length, for DAS systems this length is typically 10s of centimetres or a few metres. This becomes of significance if a phenomena of interest has a wavelength comparable to the gauge length, as peak strains may be averaged out over a longer length of structure than they may act, or localised variation in strain cannot not be detected. This is of less concern in railway infrastructure where the bending wavelengths generally exceed 3 m [21]. Simulation is used to explore the influence of gauges length on peak values. Gauge length can be reduced by increasing the intensity of backscattered light [9].

For a high-fidelity strain measurement, fibre choice plays an important role as the mechanical strain of the structure must be transferred to the fibre with minimum distortion. Coatings, jackets, or layers of armour may affect the transmission of mechanical strain from the structure to the fibre owing to slippage of the fibre within the jacket in the case of loose-tube fibre cable. On the other hand, a railway is a harsh environment for installing a sensing fibre with minimum protection, particularly during trackbed renewal. Hence, in the selection of the appropriate optical fibre for distributed sensing application, there is a trade-off between the level of mechanical transmission between the structure and the fibre and the construction of the cable surrounding the fibre. In the current study, standard telecom SMF-28 fibre with 2 mm tight-buffered jacketing was installed on the rail for curvature analysis. An armoured fibre with layers of steel and Kevlar was used in the trackbed.

Installation

A high-quality installation is essential to maximise the coupling efficiency between the fibre and the structure. Methods will depend on where the fibre is being installed and the expected behaviour of the structure or earthwork. For this technique pre-tensioning of the fibre during the installation is required for measuring compression. This depends on the amount of compression to be measured, for 500 $\mu \epsilon$ measured using a standard fibre a tension of around 0.5 N is required. Practically this can be achieved by pulling the fibre taught.

The fibre on the rail was installed while the track was closed to traffic. The fibre was temporarily held in place with soft-jaw clamps, notched to avoid crushing the fibre. This allowed the fibre to be held in tension against the rail while it was fixed in place using a quick-drying spray-on adhesive. The fibre in the trackbed was tensioned, pinned at the ends of the instrumented length and covered with sand and granular fill to hold it in place and protect it when the track was reinstated. The fibre was then held in tension by friction with the ground.

Data use

The DAS system detects changes in longitudinal strain in the fibre induced by any mechanism such as mechanical elongation and thermal expansion, although variations from thermal effects are unlikely to occur over the timescale of train passage. Measurements for the rail and subgrade were made synchronously using a connected fibre, with single interrogation unit. The location and arrangement of the sensing fibre control what is measured and which parameters can be derived from the measurements.

The fibre on the rail was arranged to capture longitudinal strain associated with rail bending. The fibre strain is a direct measurement of the rail strain, whose amplitude depends on the position of the sensing

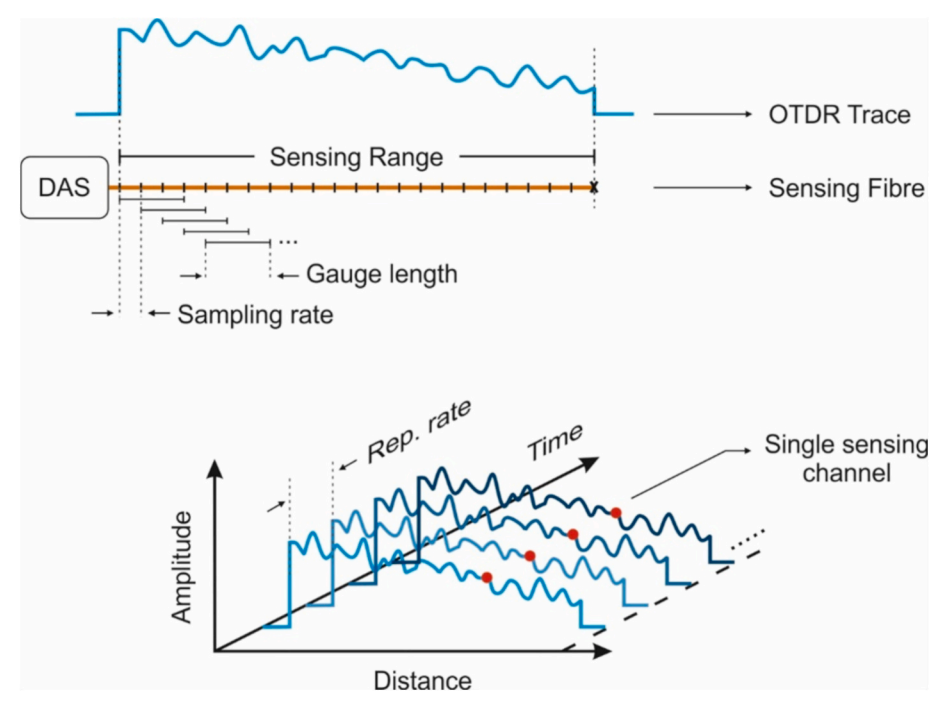


Fig. 1. Illustration of system characteristics for mechanically coupled DOFS.

fibre relative to the neutral axis of the rail. A pair of sensing fibres fixed parallel to the neutral axis strain data can be used to determine curvature. Looping the fibre back on itself on the other side of the neutral axis enables the curvature to be estimated using an optimisation procedure rather than requiring precise knowledge of the fibre positions relative to the neutral axis, which are likely to be uncertain in a field installation [13]. For rail bending, curvature is a more useful parameter than the native strain measurement as its independence of the position of the sensing fibre facilitates comparison between different locations along the rail. In general, the curvature is expected to be proportional to the applied load, and is a useful input for model based interpretations of track system behaviour [24]. For known and constant train speeds it can be related through differential equations to the kinematics of the rail and how the applied loads are distributed into the ground.

Where site and signal characteristics permit, distributed curvature data can be used to calculate low frequency rail accelerations and bending moments which, in turn, can be used to derive rail deflections and rail seat loads using bending theory. Numerically, this analysis relies on the train travelling at a steady speed. However, all the trains recorded here were accelerating away from a station. This meant it was not possible to carry out discrete load–deflection analyses reliably using the data obtained for this study, as was possible in [13].

The signal obtained from the buried fibre represents the strain in the ground associated with the deformation induced by the passage of the train. This mechanism is less explicitly defined than for rail bending and is explored in this paper. When a site is trafficked, wheel loads are distributed by the rail and transmitted through the trackbed. Under train loading, the ground will compress and the fibre will conform to the deformed shape of the ground beneath it. For a buried fibre laid longitudinally below a rail the strain in the fibre should be equivalent to the horizontal strain in the ground.

Study site and system settings

To demonstrate the installation and analysis of a longer fibre with sections buried in the trackbed, a section of plain line track near a station close to the England-Wales border was instrumented. The lightly armoured fibre was buried in the trackbed during a renewal, following the

expected line of the nearside rail (Fig. 2 (a)), and covered with a 50 mm layer of granular fill and a 9 mm thick geocomposite which were placed as part of the track renewal. Expected at a depth of 0.3 m below final sleeper level. Although 50 m of fibre was laid during the renewal work, the light armour of the fibre was not robust enough to withstand the machinery and ballast used in replacing the track, which caused the fibre to break. When the track was reinstated, only 7.5 m of the buried fibre remained intact. This indicates that a more robust fibre with stronger armour would be needed in future applications to withstand the rigours of track installation. Later, a 100 m length of sensing fibre was attached to a 50 m length of rail, above and below the rail neutral axis, nominally ± 35 mm from the rail section neutral axis (Fig. 3).

To assess the mechanical characteristics of the rail and the trackbed simultaneously, the fibre on the rail was spliced to the 7.5 m of buried fibre to form a single sensing fibre, which was then monitored using a single DAS interrogator (Fig. 2(b)). The sensing range was greater than 120 m, with a sampling rate set to 625 MHz to give 750 channels every 0.16 m, a gauge length of 0.5 m, and a temporal repetition rate of 10 kHz at which the measurement is digitised and stored. Each strain channels was high-pass filtered at 0.1 Hz to account for the thermal drift of the optical unit. The measured signals should be interpreted in the context of potential artefacts from signal processing and the characteristics of the measurement system. Reducing the gauge length and increasing the laser stability will reduce the influence of these artefacts.

Measurements were made as the site was trafficked by two classes of trains (Class 170 and Class 150) as they accelerated away from the station; hence speeds were generally low ($<30\,\mathrm{km/h}$). The Class 170 and Class 150 trains have expected wheel loads of 60–65 kN and 45–50 kN (depending on occupancy) and vehicle lengths of 23 m and 20 m, respectively. Signals from the different portions of fibre were identified, then aligned by cross-correlation for the loading event.

Supporting measurements

The fibre was installed at the study site along with a host of other instruments such as pressure cells and accelerometers for evaluating the performance of the site [7]. The optical system was trialled as a new experimental technique which involved increased train speeds,



Fig. 2. Site 1 (a) buried fibre, (b) final installation (c) buried instrumentation.

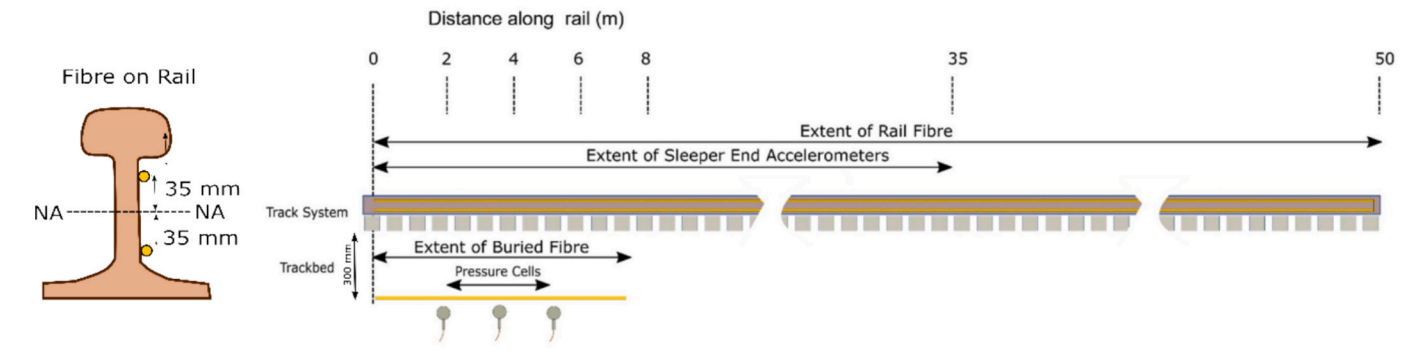


Fig. 3. Site plan, detailing extents of sensing fibres and complementary instrumentation.

increased fibre length, and burial of the fibre. Additional data obtained using established measurement methods was used to support interpretation and validate the DAS signal, these are described and reported here.

Established instrumentation was installed at the site comprised sleeper end accelerometers and pressure cells placed at the ballast subgrade interface (Fig. 2 (c)), to quantify the site behaviour and track system properties. The arrangement of the conventional instrumentation and the optical fibre is shown in Fig. 3. All distances were measured relative to the first accelerometer, which was placed to coincide with the start of the mechanically coupled portion of the optical fibre.

Characteristic sleeper deflections are mapped along the nearside rail of the site in Fig. 4. These were obtained using sleeper end accelerometers, by filtering and integrating twice, i.e. the same sensors and analysis methods described in [11]. The deflections are fairly uniform along the length of the site (Table 2). Some variation from sleeper to sleeper is apparent, and there is a general reduction in deflection from 20 m onwards, but there are no significant voids of soft spots.

 Table 2

 Sample moments for sleeper deflection and support system modulus.

	Deflection (mm)	Support System Modulus (MN/m ²)
Mean	0.8	23
Standard Deviation	0.2	3

Fig. 5 shows the results from the pressure cells at different distances along the length of the fibre, buried at the top of the subgrade and covered by the same granular fill and geotextile as the fibre. These sensors were located vertically below the rail seat. The peaks in pressure associated with the passage of each wheelset are clear. The pressure cells do not fully unload between successive wheels on a bogie, or between the bogies at the ends of adjacent vehicles, indicating interaction between these wheelsets. The peak loads vary along the track and from wheel to wheel.

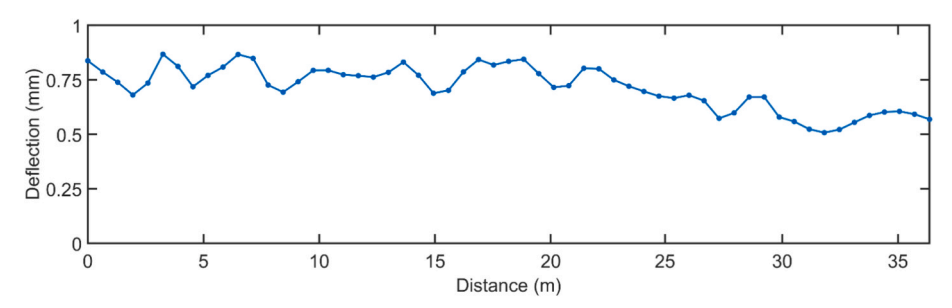


Fig. 4. Average sleeper deflection along the study site obtained from acceleration measurements during the passage of 5 class 175 trainsets.

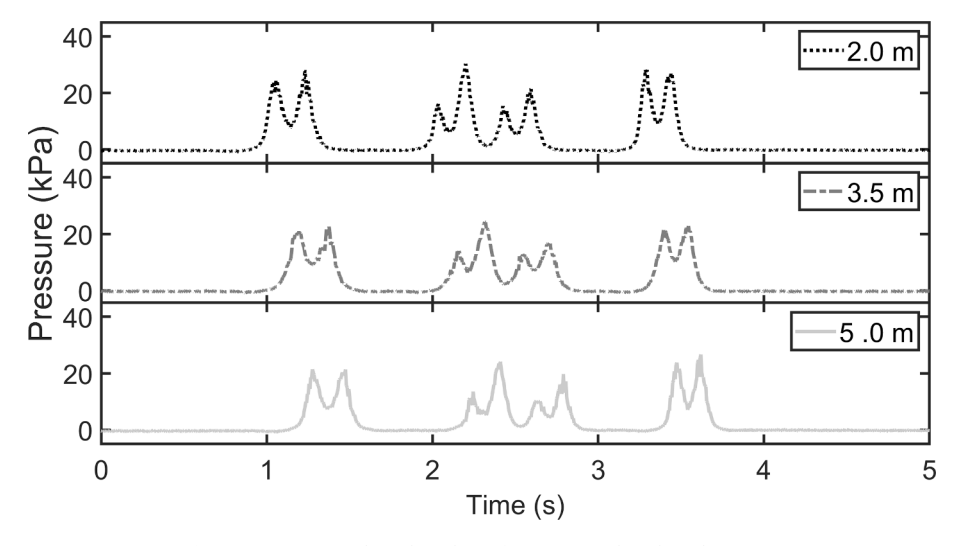


Fig. 5. Pressures at the subgrade surface measured at three locations.

Numerical simulation

Alongside the measurements, a static simulation of the interaction between the train, track, and ground with and without a fibre was undertaken. The simulation involved a simplified elastic analysis for static wheel loading, from a pair of bogies at the vehicle ends, carried out using ABAQUS.

The purpose of the model was to simulate the behaviour of a buried sensing fibre under representative train loading and typical site conditions to contextualise and aid interpretation of the signal, rather than to reproduce the measured behaviour exactly. A static analysis is sufficient for this purpose as the moving static load is likely to be the dominant loading effect, and the behaviour along the track at an instant in time should reflect that at a single location being passed by a train moving along the track, for near-uniform support conditions.

The rail and sensing fibre were modelled as beam elements, and the ballast and other trackbed layers as elastic solids. The fibre was embedded in the centre of the fill layer. The geocomposite was omitted from the simulation. The wheel spacings, loads and material parameters for the track, trackbed and optical fibre are given in Table 3. These parameters result in a track support system modulus of $23 \, \text{MN/m}^2$, close to the average value indicated for the site in Fig. 4(b).

Fig. 6 shows a vertically exaggerated visualisation for the simulated track deformations for the static train loads along the track. The sleeper deflections beneath the wheel loads are about 0.8 mm. This is close to the average measured deflection at the site in Fig. 4(a), indicating that the model is broadly representative of this aspect of system behaviour.

Fig. 7 shows the calculated strain along the fibre for the element

Table 3Summary of parameters used in the simulation.

Component	Parameter	Value
Train	Wheel load	65 kN
	Wheel spacing, Bogie spacing	2.6 m, 7.6 m (Class 175)
56 kg Rail	Bending stiffness	4.9 MNm ⁴
Rail Pad	Pad stiffness	280 MN/m
Ballast	Layer thickness	0.25 m
	Young's Modulus	150 MN/ m^2
Fill	Layer thickness	0.1 m
	Young's Modulus	200 MN/ m ²
Subgrade	Layer thickness	15.65 m
	Young Modulus	$30 + 7z \text{ MN/m}^2$
Optical Fibre	Fibre diameter	125 μm
	Young's Modulus	70 GN/m ²
	Burial Depth	0.3 m below sleeper base
All Materials	Poisson's Ratio	0.3

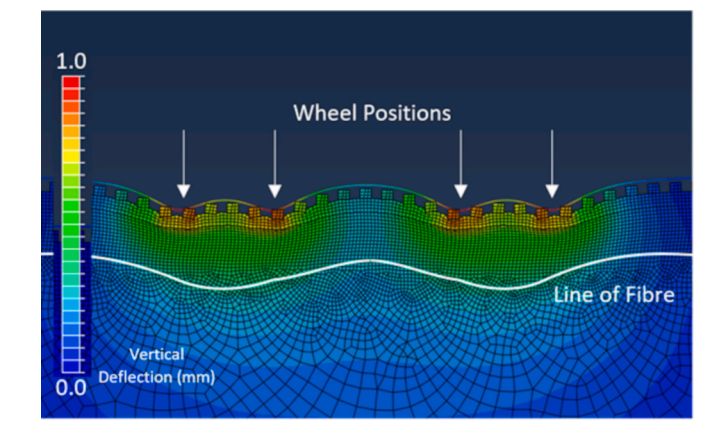


Fig. 6. Finite element simulation of track with buried optical fibre under static wheel loads in Abagus.

length used in the simulation (0.1 m) and the same result filtered to be representative of the actual optical fibre gauge length (0.5 m). Fig. 7 shows that.

- the fibre experiences tension and compression along its length as the ground deforms,
- the horizontal strains simulated for the fill layer are the same as those found for the fibre,
- peak strain is expected to be greatest beneath the train wheels, and
- interaction occurs between wheel loads.

The simulation indicates that a buried fibre will provide a measurement of horizontal strain in the ground along an infrastructure. The results also show how increasing the gauge length will lead to a reduction in the observed peak strain.

Results

Fibre on the rail

Results are presented in Fig. 8 for the two train types: (a) the longer, heavier Class 175/0 and (b) the shorter, lighter Class 150/2. Both trains comprise two vehicles and were accelerating away from the station, with speeds increasing from 5.6 to 7.6 m/s and from 6.8 to 8.2 m/s respectively. At 20 to 30 km/h, these are marginally faster than most previous

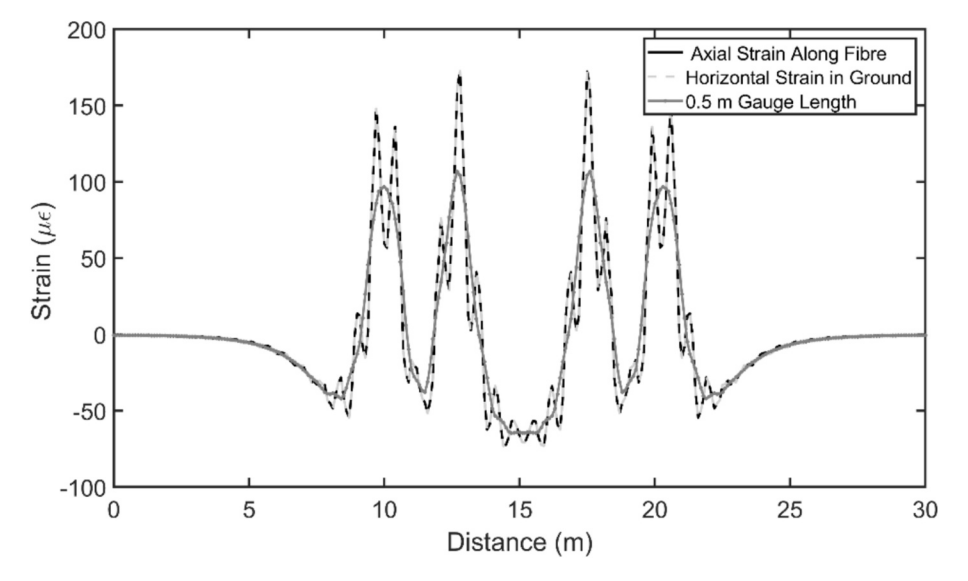


Fig. 7. Simulated strain along a buried fibre.

studies.

Fig. 8 shows the curvature determined from strain measurements along the full 50 m length of rail for the complete passage of each train. The velocity and acceleration of the train is manifest in the shape of the wavefronts associated with successive wheels of the train, which could be analysed using the equations of motion. At low speeds, the curvature would be expected to be directly proportional to the applied loading (as would the rail strain for the same measurement position). The mean ratio of the peak curvature along the fibre (associated with the central bogie pairs) between the two train types is about 0.75. This is indeed close to the ratio of the vehicle weights, which are expected to be about 48 tonnes and 36 tonnes for the Class 175 and 150 trains, respectively.

With distributed curvature data it is possible to effectively follow a near constant load along the track: Fig. 9 shows the maximum and minimum curvature associated with the central bogie pair from Fig. 8 (a). In general, the peak curvature increases up to 20–25 m along the site. This curvature characteristic agrees with the reduction in defection observed in Fig. 4, as both indicate stiffer track, which leads to lower amplitude but narrower deflection bowls [21].

Fig. 10 compares the simulated curvature, filtered to account for the 0.5 m gauge length, with the measured curvature for the first 25 m of fibre at a time t=6 s from Fig. 8a for the central bogie pair of the train. These are a similar order of magnitude $(10^{-3}m^{-1})$ to those observed in other field studies [14,20], only with smaller amplitudes corresponding to the small track deflections.

Given that no attempt has been made to tune the simulation to replicate the data, the agreement is generally good. The minima in the curvature correspond to the wheels of the train, the orders of magnitude of the curvature are the same and the signal shape is broadly the same. The measurement is noisier, more variable, and has a lower resolution, as would be expected with a simple and uniformly parameterised simulation.

Buried fibre

The portions of the signal for the 7.5 m length of track where both the rail and subgrade were instrumented were extracted and aligned using cross correlation. The results are shown in Fig. 11 for the same trains as before (Class 175 and Class 150), for the rail above the neutral axis and the trackbed. The lighter class 150 gives a lower signal-to-noise ratio.

Data for the rail in Fig. 10 were recorded around 35 mm above the neutral axis, hence the rail (and fibre) are in compression under wheel loading. The subgrade fibre is in tension when under load, which would

be expected and is consistent with the simulation (Fig. 7). The progression of peaks associated with the wheels of the train is apparent for both trains at both positions in the track system. This implies that the signal from the buried fibre could be suitable for train detection and speed estimation, although this can be done using "dark" fibres running alongside the track. The purpose of a dedicated, mechanically-coupled fibre is to allow quantitative measurement and mechanistic analysis of actual system behaviour including how vehicle loads are distributed into the ground and the impact of different wheel loads.

The strains measured on the rail, above the neutral axis are [inversely] correlated with those measured in the subgrade. The strains for the heavier train are greater than those for the lighter train at the same location, as would be expected.

The measurements can be analysed to show how the wheel loads are distributed into the track. In Fig. 11, the bands of high intensity strain associated with the progression of wheels are broader for the subgrade than for the rail. This can be analysed further by computing the Fourier transform to the frequency domain at every measurement point along the fibre to assess whether the dominant frequencies change and the Fourier transform to the wavenumber domain at every instant in time during train passage to assess the lengths that loads are carried over. The amplitudes normalised by the peak for each spectrum are shown in Fig. 12 for both locations, using the data for the heavier Class 175 from Fig. 11a. Wavenumber being the reciprocal of the wavelength, which in this case are the lengths associated with bending of the rail and deformation of the ground.

Both at the rail and in the trackbed, the frequencies that dominate the frequency spectrum depend on the arrangement of wheels within the train loading the track [1,12]and the wavenumbers depend on the widths of the deflection basins and interactions between individual wheels. At the rail, the effects from individual wheels are expected to be more pronounced than at depth, where the vehicle ends (bogie pairs) dominate [17]. This should manifest as an increase in the lower frequency content of the spectrogram (although the dominant frequencies do not change) and a shift to lower wavenumbers (longer wavelengths). This can be seen in Fig. 12 ((a&c) for frequency and (b&d) for wavenumber), as would be expected from elastic theory [16,25].

Strain time-histories at distances of 2.0, 3.5 and 5.0 m along the buried fibre are shown in Fig. 13, close to the pressure cells (Fig. 5) for a Class 175. The measurements (Fig. 13) and the simulation (Fig. 7) both show peaks in fibre tension corresponding to interacting wheelsets of the same order of magnitude (\sim 100 μ e). Generally, the agreement between the shape of the signal for the simulation and the measurements is good,

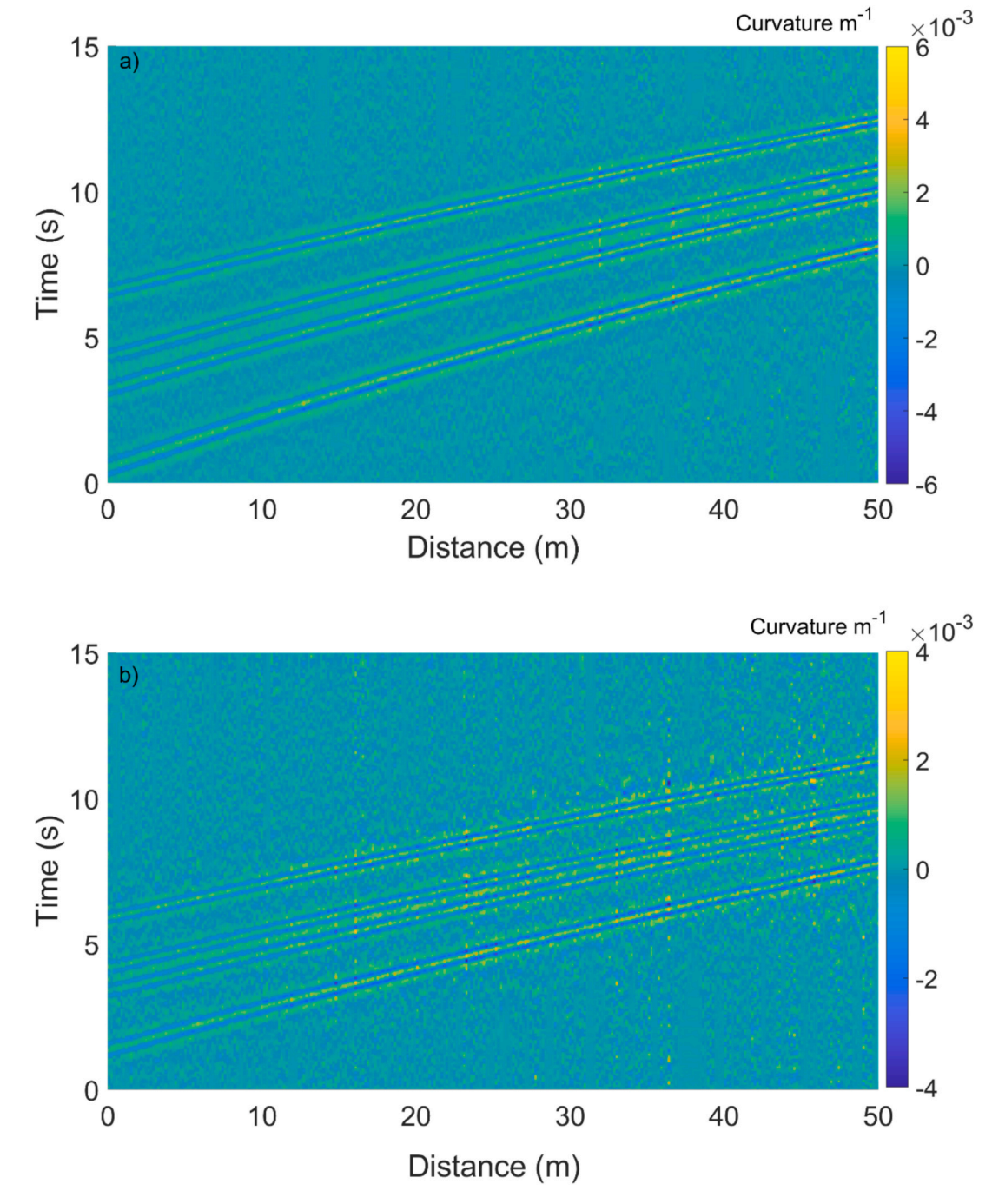


Fig. 8. Distributed curvature for (a) class 175 and (b) a class 150 train.

particularly when the gauge length of the fibre is accounted for. This indicates that the fibre is providing a measurement of the horizontal strain (hence stress) in the ground, for wavelengths longer than the gauge length.

At the locations where the pressure cell data, shown in Fig. 5, indicated higher pressures during the passage of the train, the buried fibre experienced lower strain and vice-versa. This is because, as shown by simple track models, stiffer track support increases load concentration (hence higher loads are detected by a pressure cell), but the stiffer ground deforms less, leading to reduced strain in a mechanically coupled fibre.

The measured strain signal for a buried fibre is of the form expected from the simulation and has a linear relationship with the effect being monitored, as intended. The analyses presented here illustrate the

potential for buried fibres to measure the response of the ground to different magnitudes and geometries of applied loading, detect localise stiffness variation, and investigate changes in load distribution at depth. However, the obtained signal in this example depends on the interactions between the vehicle, the track system, and the ground. While this potentially contains a variety of information about the infrastructure and applied loading, different variables such as fibre depth, traffic type, and soil layers, would need to be controlled or accounted for to enable more analytical and detailed interpretations.

Conclusions

This study has demonstrated the application of a mechanically coupled sensing fibre deployed on an operational railway. A continuous

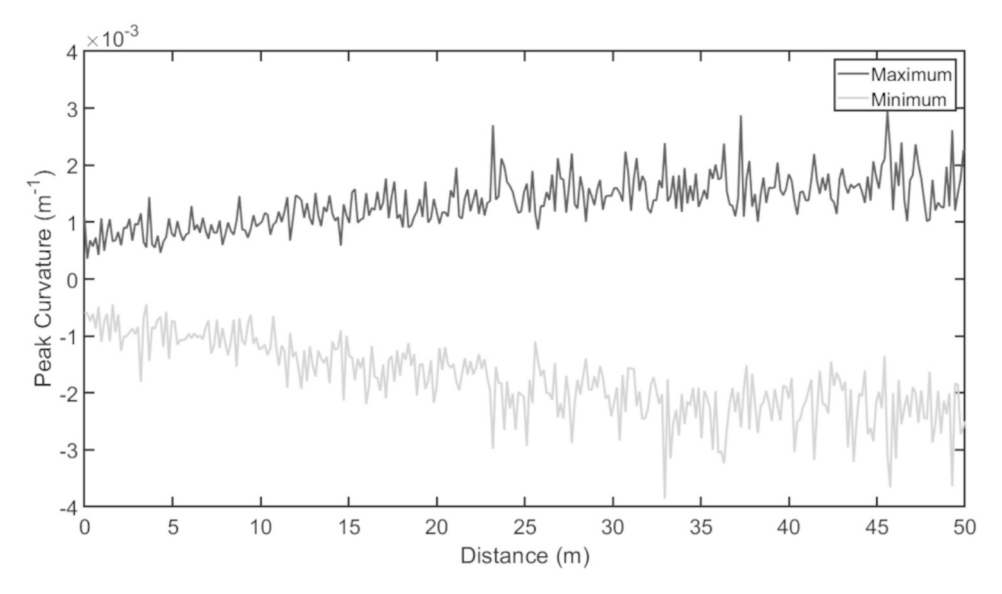


Fig. 9. Maximum and Minimum Curvature along the Rail.

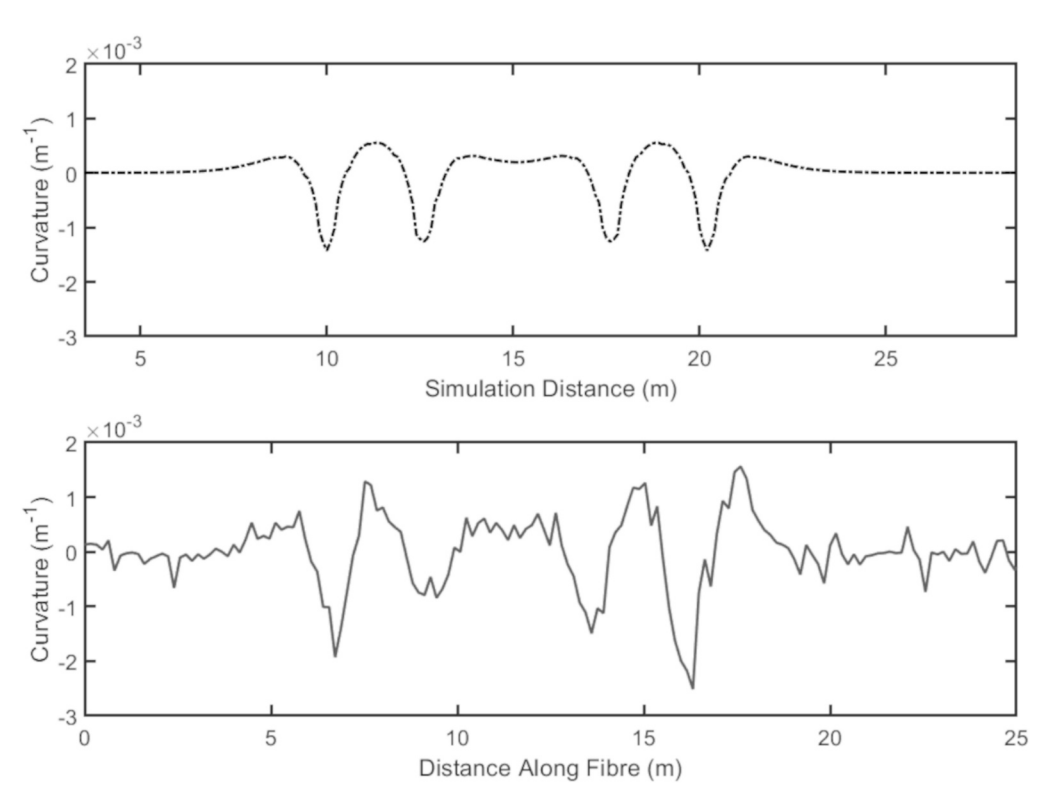


Fig. 10. (a) Simulated and (b) measured curvature along the fibre at $t=6\ s$.

sensing fibre, covering 50 m of rail and 7.5 m of the trackbed, was interrogated using a DAS interrogator to measure strains caused by passing trains. This was a large-scale field trial, and the system could be used for measurement along kilometres of track, earthwork or other infrastructure. A dedicated sensing fibre with a specific arrangement and an interrogator capable of high sampling rates for a short gauge length means the technique can be used for granular quantitative measurement rather than merely qualitative monitoring or detection.

Optical fibre measurements, simulation, and data from established measurement methods have provided insights into the measurement principle, expected signal form, and external variables relevant for a DOFS mechanically coupled or embedded in transport infrastructure.

Specifically:

- The data produced by distributed optical fibres are of a similar form to the outputs of established simulation techniques. For the loading of the railway track, the measured data were of the form expected from the simulation, for fibres both on the rail and buried in the trackbed. This suggests that the measurements have the potential to be interpreted analytically. Shorter gauge lengths and improved thermal stability should, in principle, enhance this sensing technique for mechanical applications.
- DOFS mechanically coupled to structures provide a direct measurement of the strain experienced by that structure. For simple

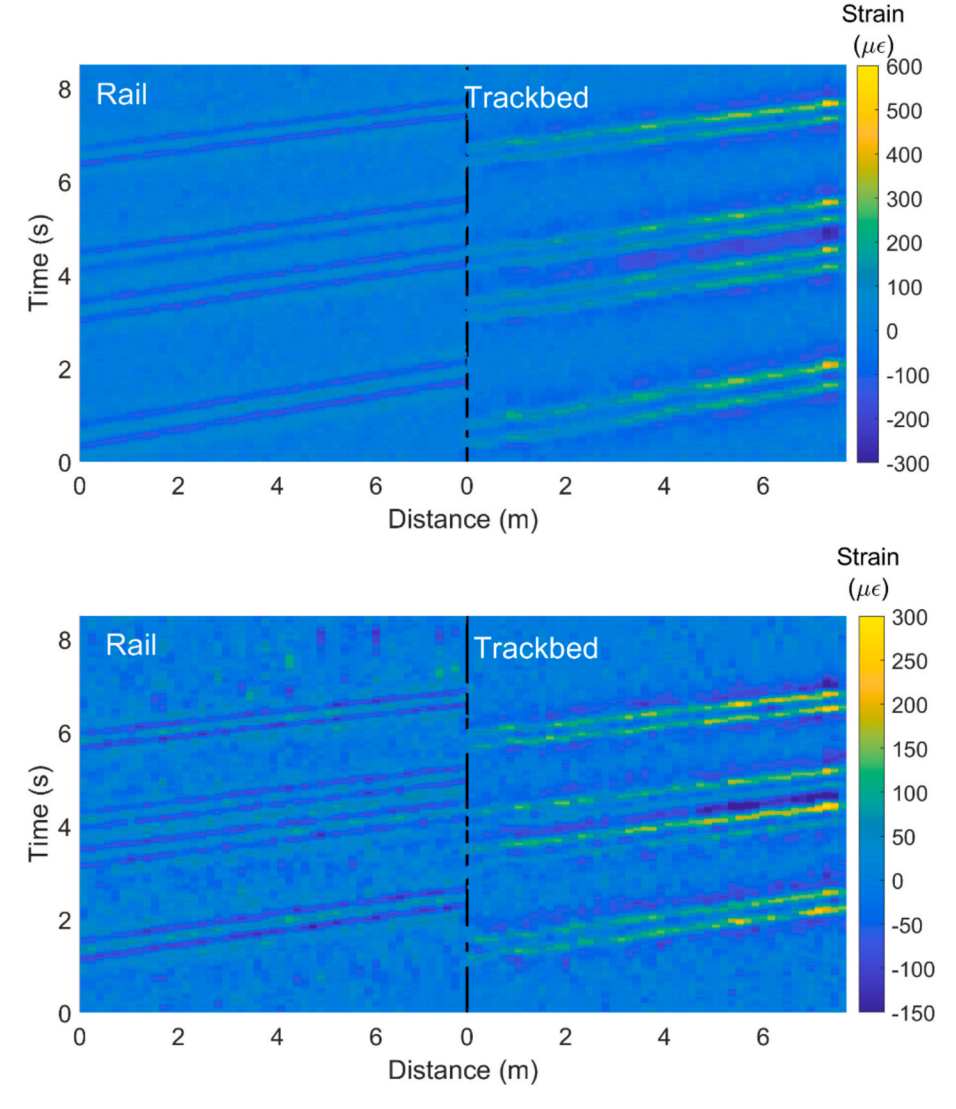


Fig. 11. Rail and subgrade strain (a) for a class 175 (b) for a class 150.

structures such as a steel rail, the sensing fibre can be arranged to measure curvature and derive other quantities. The responses for different load magnitudes confirm the expected linearity of the measurement system.

- A fibre buried longitudinally along a piece of infrastructure can provide a measurement for horizontal strain, that indicates how ground deforms as it distributes the applied loading at depth.
- Vehicle loading is an interaction, this means that the measured quantities depend on the material properties variation and layering in the ground, interactions between loads as well as the depth of burial.

Understanding and being able to account for these factors will increase the potential for DOFS for quantitative measurement and monitoring purposes in transport infrastructure.

Research data

Data used for this study are available from the University of Southampton data repository at: https://doi.org/10.5258/SOTON/D3518.

Funding sources

This research was supported by the European Union Research and

Innovation project In2Track2 S2R-CFM-IP3-01-2018, co-ordinated by Network Rail and Natural Environment Research Council Grants NE/S012877/1 and NE/T005890/1.

CRediT authorship contribution statement

David Milne: Writing – original draft, Software, Project administration, Methodology, Investigation, Funding acquisition, Formal analysis, Data curation. Ali Masoudi: Writing – original draft, Software, Methodology. John Harkness: Writing – review & editing, Software, Investigation. Ben Lee: Writing – review & editing, Project administration, Investigation, Funding acquisition. Geoff Watson: Writing – review & editing, Investigation. Louis Le Pen: Investigation, Funding acquisition. Gilberto Brambilla: Resources. William Powrie: Writing – review & editing, Resources, Funding acquisition.

Declaration of competing interest

The authors declare the following financial interests/personal relationships which may be considered as potential competing interests: [David Milne reports financial support was provided by Network Rail Ltd. If there are other authors, they declare that they have no known competing financial interests or personal relationships that could have appeared to influence the work reported in this paper].

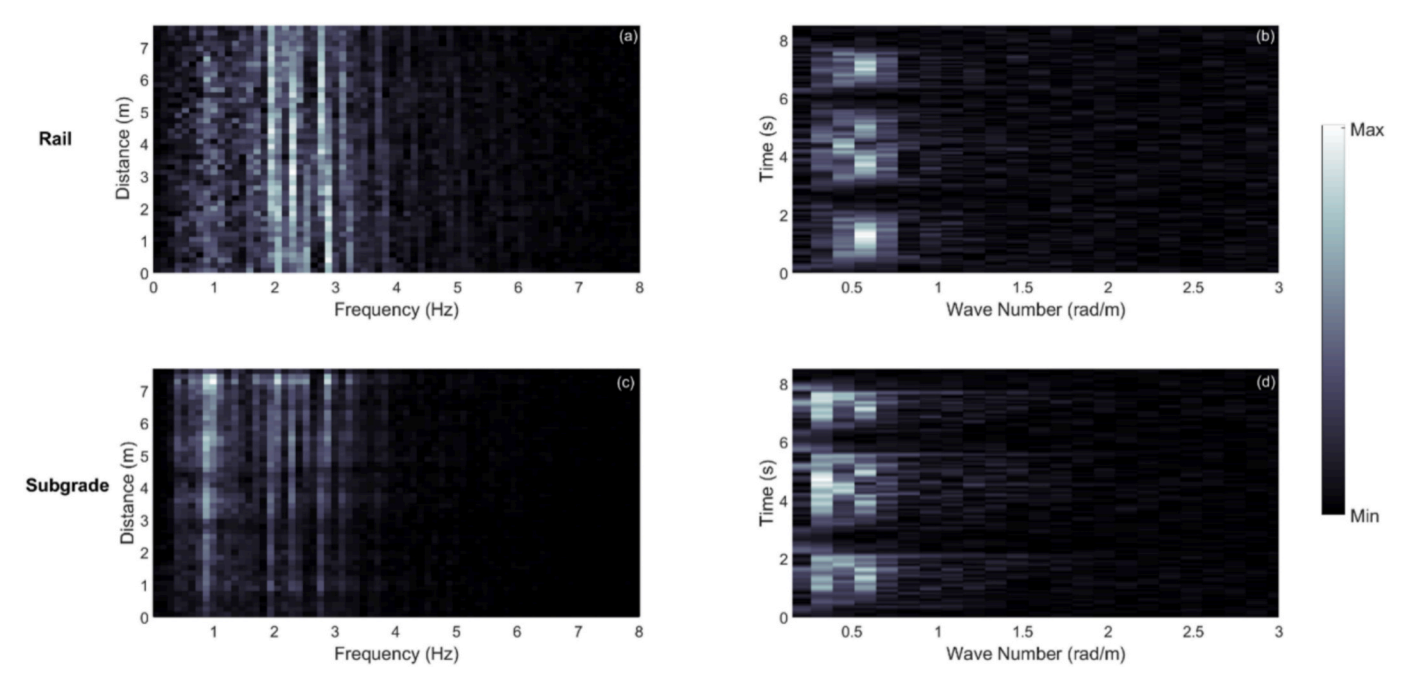


Fig. 12. Normalised Intensity maps for the Fourier transforms into the (a) frequency domain and (b) wave number domain for the rail and (c) frequency domain and (d) wave number domain for the subgrade fibre for the class 175.

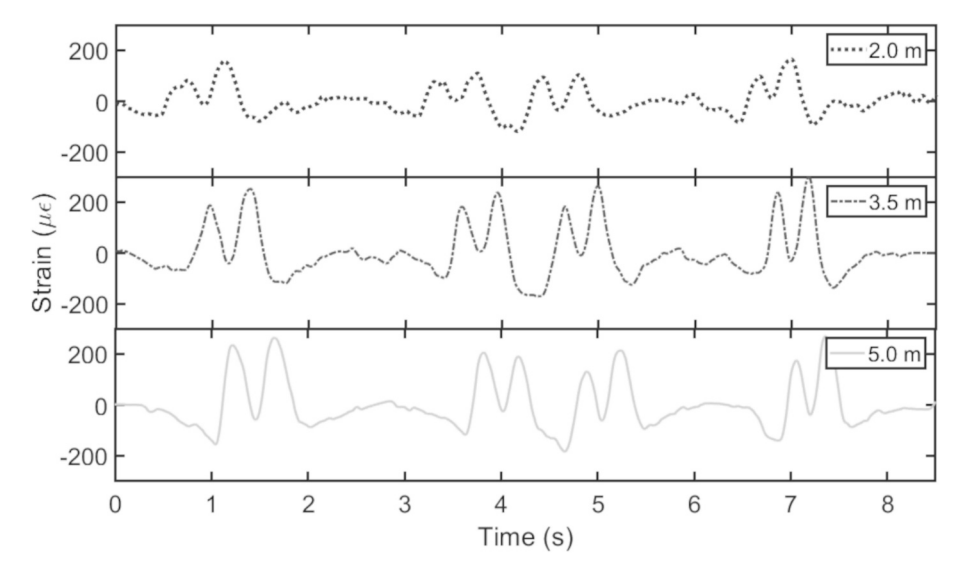


Fig. 13. Strain-time histories for three locations along the buried fibre for the central bogies of a class 175 train.

Data availability

Data are publically available from a University of Southampton Repository https://doi.org/10.5258/SOTON/D3518

References

- Auersch L. The excitation of ground vibration by rail traffic: theory of vehicle-track-soil interaction and measurements on high-speed lines. J. Sound Vib. 2005;284(1-2):103-32.
- [2] Bakhtiari Gorajoobi S, Masoudi A, Brambilla G. Long range raman-amplified distributed acoustic sensor based on spontaneous brillouin scattering for large strain sensing. Sensors 2022;22(5):2047.
- [3] Castillo-Mingorance JM, Sol-Sánchez M, Moreno-Navarro F, Rubio-Gámez MC. A critical review of sensors for the continuous monitoring of smart and sustainable railway infrastructures. Sustainability 2020;12(22):9428.
- [4] Cedilnik G, Lees G, Schmidt PE, Herstrøm S, Geisler T. Pushing the reach of fiber distributed acoustic sensing to 125 km without the use of amplification. IEEE Sens. Lett. 2019;3(3):1–4.

- [5] Du C, Dutta S, Kurup P, Yu T, Wang X. A review of railway infrastructure monitoring using fiber optic sensors. Sens. Actuators, A 2020;303:111728.
- [6] Hartog AH. An introduction to distributed optical fibre sensors. CRC Press; 2017.
- [7] In2Track2 (2021) D4.3 Development of next generation track sub-structure treatments.
- [8] Masoudi A, Belal M, Newson T. A distributed optical fibre dynamic strain sensor based on phase-OTDR. Meas. Sci. Technol. 2013;24(8):085204.
- [9] Masoudi A, Beresna M, Brambilla G. 152 km-range single-ended distributed acoustic sensor based on inline optical amplification and a micromachined enhanced-backscattering fiber. Opt. Lett. 2021;46(3):552–5.
- [10] Masoudi A, Newson TP. High spatial resolution distributed optical fiber dynamic strain sensor with enhanced frequency and strain resolution. Opt. Lett. 2017;42(2): 290–3.
- [11] Milne D, Harkness J, Le Pen L, Powrie W. The influence of variation in track level and support system stiffness over longer lengths of track for track performance and vehicle track interaction. Veh. Syst. Dyn. 2019:1–24.
- [12] Milne D, Le Pen LM, Thompson DJ, Powrie W. Properties of train load frequencies and their applications. J. Sound Vib. 2017;397:123–40.
- [13] Milne D, Masoudi A, Ferro E, Watson G, Le Pen L. An analysis of railway track behaviour based on distributed optical fibre acoustic sensing. Mech. Syst. Sig. Process. 2020;142:106769.

- [14] Pannese EM, Take WA, Hoult NA, Yan R, Le H. Bridge transition monitoring: Interpretation of track defects using digital image correlation and distributed fiber optic strain sensing. Proceed. Ins. Mech. Eng., Part F: J. Rail and Rapid Transit 2020;234(6):616–37.
- [15] Parajuli B, Gharizadehvarnosefaderani M, Damm D, Rabbi MF, Drapp B, Pooch A, et al. Rail track support condition monitoring with distributed acoustic sensing (DAS) system. Proceedings of the Institution of Mechanical Engineers, Part F: Journal of Rail and Rapid Transit. 2025.
- [16] Poulos HG, Davis EH. Elastic solutions for soil and rock mechanics. Wiley; 1973.
- [17] Powrie W, Le Pen L, Milne D, Thompson D. Train loading effects in railway geotechnical engineering: Ground response, analysis, measurement and interpretation. Transp. Geotech. 2019;21:100261.
- [18] Rahman MA, Taheri H, Dababneh F, Karganroudi SS, Arhamnamazi S. A review of distributed acoustic sensing applications for railroad condition monitoring. Mech. Syst. Sig. Process. 2024;208:110983.
- [19] Sun F, Hoult NA, Butler LJ, Zhang M. Field monitoring and prediction of the thermal response of an in-service curved continuous welded rail using distributed fiber optic strain measurements. J. Civ. Struct. Heal. Monit. 2025;15(4):1025–39.

- [20] Sun F, Hoult Neil A, Butler L, Zhang M. Dynamic monitoring of rail behavior under passenger train loading using distributed fiber optic sensors. J. Perform. Constr. Facil 2024;38(4):04024018.
- [21] Timoshenko S, Langer BF. Stresses in railroad track. ASME Trans. 1932;54:277-93.
- [22] Vidovic I, Marschnig S. Optical fibres for condition monitoring of railway infrastructure—encouraging data source or errant effort? Appl. Sci. 2020;10(17): 6016
- [23] Wheeler LN, Pannese E, Hoult NA, Take WA, Le H. Measurement of distributed dynamic rail strains using a Rayleigh backscatter based fiber optic sensor: Lab and field evaluation. Transp. Geotech. 2018;14:70–80.
- [24] Wheeler LN, Take WA, Hoult NA, Le H. The use of fiber optic sensing to measure distributed rail strains and determine rail seat forces due to a moving train. Can. Geotech. J. 2018.
- [25] Yang LA, Powrie W, Priest JA. Dynamic stress analysis of a ballasted railway track bed during train passage. J. Geotech. Geoenviron. Eng. 2009;135(5):680–9.